ELSEVIER

Surface and Coatings Technology 78 (1996) 211–218

SURFACE & COATINGS TECHNOLOGY

Ion nitriding of titanium aluminides with 25–53 at.% Al I: Nitriding parameters and microstructure characterization

C.L. Chu, S.K. Wu

Institute of Materials Science and Engineering, National Taiwan University, Taipei 106, Taiwan

Received 25 July 1994; accepted in final form 28 November 1994

Abstract

Titanium aluminides with Al contents of 25, 40, 50 and 53 at.% were ion nitrided to modify the surface conditions. The effects of four process parameters, namely nitriding temperature, nitriding time, working pressure and $[N_2]/[H_2]$ ratio, were investigated by the orthogonal test. The phases and microstructures of the nitrided surface were studied by X-ray diffraction (XRD), electron probe microanalysis, optical microscopy and scanning electron microscopy. Experimental results indicate that nitriding temperature and time are the primary parameters responsible for improving surface hardness. The nitrided compound layer consists of TiN and Ti_2AlN phases. As the Al content in titanium aluminides increases, the XRD intensity of Ti_2AlN phase becomes stronger. The diffusion layer in all the cases has little nitrogen, allowing this layer to be easily attacked by the etching reagent. A mechanism to explain the formation of the ion-nitrided layer in titanium aluminides is also proposed in this study.

Keywords: Ion nitriding; Titanium aluminides; Orthogonal testing; TiN; Ti_2AlN

1. Introduction

Titanium aluminides have attracted a great deal of research interest because of their potential for high temperature applications; however, their low surface hardness restricts their tribological applications. Nitriding techniques are commonly used to improve the fatigue and wear resistance of metals and alloys [1]. In particular, ion nitriding has a number of advantages over conventional nitriding including faster growth rates of nitrided layers, easier control over the crystal structure of nitrided layers, and fewer environmental problems [2]. Several investigations on ion nitriding have been done for titanium and titanium alloys [3–14], but so far there have been few investigations on titanium aluminides. Only the effects of ion nitrogen implantation on titanium aluminides has been reported [15–17]. In the present work, the ion nitriding of titanium aluminides containing 25–53 at.% Al is investigated. The nitriding parameters and the characteristics of the nitrided layers are discussed.

2. Experimental details

A conventional tungsten arc melting technique was employed to prepare titanium aluminides containing 25, 40, 50 and 53 at.% Al. Titanium (purity, 99.7%) and aluminium (purity, 99.99%), totaling 100 g, were melted and remelted at least six times in an argon atmosphere. Pure titanium buttons were also melted and used as getters. The mass loss during melting was negligible. The as-melted buttons were homogenized at 1050 °C in a 7×10^{-6} Torr vacuum furnace for 4 days. Specimens with dimensions of 10 mm × 20 mm × 1 mm were then cut from the homogenized buttons using a low speed diamond saw. A hole, 2.5 mm in diameter, was drilled in each specimen by electrical discharge machining. This hole was used to hang the specimen during the ion nitriding. The specimen surface was then polished with 1000 grit emery paper. Before ion nitriding, all specimens were cleaned ultrasonically in acetone to remove surface grease.

Ion nitriding was carried out in a NDK furnace model JIN-6SS-C-SV. The specimen's support and holder were made of titanium to reduce contamination of the specimen surface during the sputtering process. After nitriding, the specimens were cooled in a vacuum. In order to investigate the relation between treatment parameters and surface properties, four treatment parameters were considered: nitriding temperature, nitriding time, working pressure, and nitrogen-to-hydrogen ratio ($[N_2]/[H_2]$ ratio). According to the standard L9 orthogonal arrays,

SSDI 0257-8972(94)02411-1

Table 1
Nitriding parameters employed in the L9 orthogonal test

Experiment	Nitriding temperature (°C)	Nitriding time (h)	Working pressure (Torr)	$[N_2]/[H_2]$ ratio
1	700	4	6	10
2	700	12	8	4
3	700	24	10	1
4	800	4	8	1
5	800	12	10	10
6	800	24	6	4
7	900	4	10	4
8	900	12	6	1
9	900	24	8	10

the experimental data were analyzed using the analysis of variance (ANOVA) technique [18]. The standard L9 orthogonal arrays used in this study are listed in Table 1.

The microstructures of the nitrided layers were studied by X-ray diffraction (XRD), optical microscopy (OM) and scanning electron microscopy (SEM)–energy-dispersive X-ray analysis (EDXA). XRD tests were carried out on a Philips PW1710 X-ray diffractor using Cu Kα radiation. The power was 40 kV × 30 mA and the 2θ scanning rate was $3^\circ\ min^{-1}$. The surface hardness was tested with a micro-Vickers tester with a load of 25 gf for 15 s. For each specimen, at least five different locations were tested. The surface morphologies of ion-nitrided samples were observed by OM. They were then sectioned with a low speed diamond saw and mounted on edge to observe the cross-section with a Philips 515 scanning electron microscope with EDXA facility. The chemical composition of surface layers was analyzed using a JEOL JXA-8600SX electron probe microanalyzer.

3. Results and discussion

3.1. Effect of treatment parameters on the ion nitriding of titanium aluminides

Fig. 1 shows the response diagrams by ANOVA analysis [18] of the S/N variation of surface hardness. The S/N value indicates the relationship of the factor levels to surface hardness, the higher S/N value corresponding to better treatment parameters. For example, in Fig. 1(a), treatment at 900 °C for 24 h, 6 Torr and $[N_2]/[H_2]=1$ leads to the greatest surface hardness for the Ti–25Al alloy (where the composition is in atomic per cent). At the same time, Fig. 1 also shows that the nitriding temperature and nitriding time have a greater effect on the surface hardness than do the $[N_2]/[H_2]$ ratio and working pressure. However, the original Al content in the specimen has little effect on the S/N variation. For example, the S/N variation in the surface hardness for

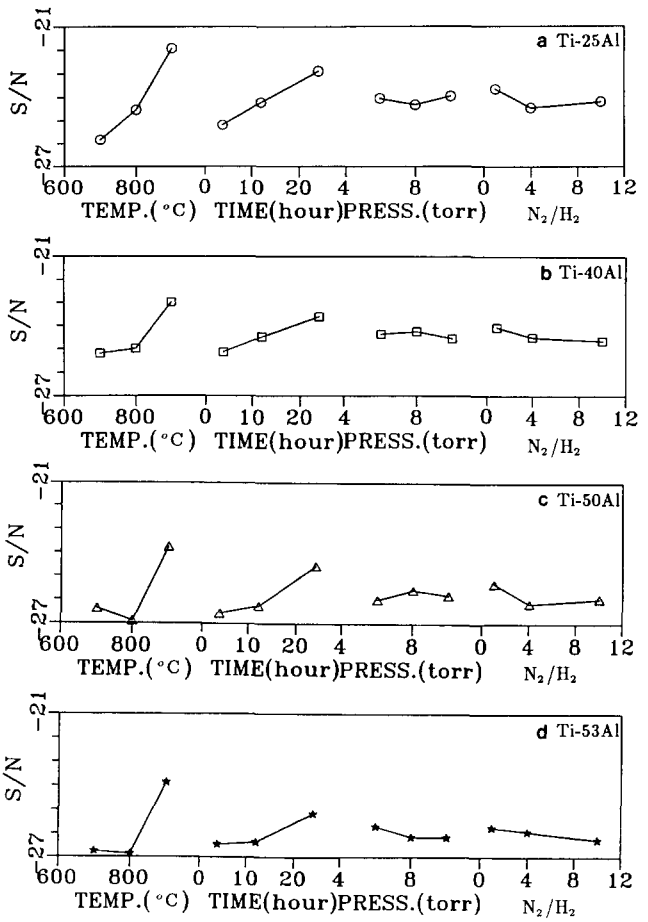

Fig. 1. S/N variation of surface hardness of (a) Ti–25Al, (b) Ti–40Al, (c) Ti–50Al and (d) Ti–53Al alloys using an L9 orthogonal array as shown in Table 1.

Ti–25Al is larger than those for Ti–50Al and Ti–53Al, as shown in Fig. 1.

In order to investigate the single-parameter effects on the surface hardness of the nitrided layer, standard treatment levels for temperature, time, working pressure and $[N_2]/[H_2]$ ratio were set at 900 °C, 12 h, 8 Torr and 10 respectively. One parameter was then varied while the others were kept at their standard level. The test results are shown in Fig. 2. For all specimens, the surface hardness increases with increasing nitriding temperature and nitriding time but decreases or has no obvious effect with increasing working pressure and $[N_2]/[H_2]$ ratio. In Fig. 2, some error in the measured hardness values may occur since penetration depths of the indentation may exceed the thickness of nitrided layers.

3.2. Microstructures of ion-nitrided titanium aluminides

After ion nitriding, the specimens' surface shows a different color, ranging from brown to golden yellow, which depends on nitriding parameters and Al content in the specimen.

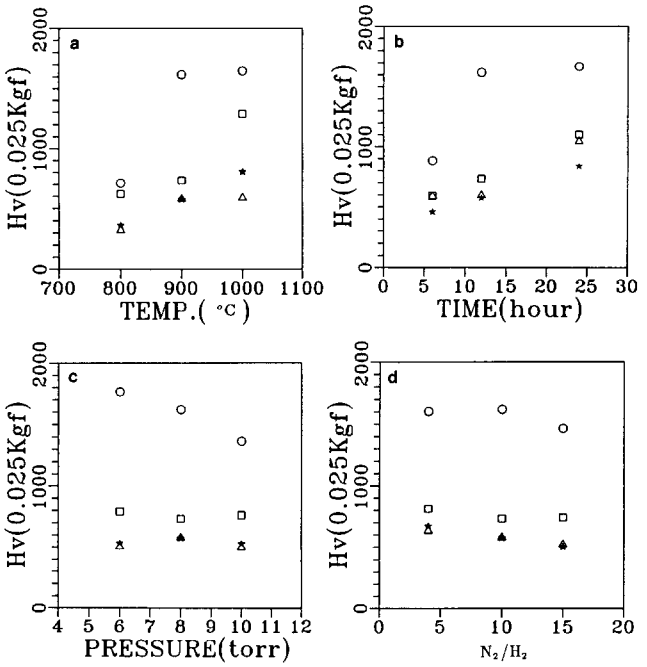

Fig. 2. Surface hardness of titanium aluminides ion nitrided at 900 °C for 12 h and 8 Torr with $[N_2]/[H_2]=10$ for various (a) nitriding temperatures, (b) nitriding times, (c) working pressures and (d) $[N_2]/[H_2]$ ratios. ○ Ti–25Al; □ Ti–40Al; △ Ti–50Al; ★ Ti–53Al.

Typical cross-section micrographs of the nitrided titanium aluminides after treatment at 1000 °C for 12 h are shown in Figs. 3 and 4. Fig. 3 shows the optical micrographs. On carefully examining Fig. 3, one can see that a white layer is formed which is hardly attacked by the etching reagent (5% hydrofluoric acid, 10% nitric acid and 85% H_2O). This layer is the compound layer, as is often seen in nitrided pure titanium and its alloys [3–14]. The original microstructure of titanium aluminide before ion nitriding also can be seen in Fig. 3. Fig. 4 shows the scanning electron micrographs. Secondary-electron images are shown in Fig. 4(a) and backscattered-electron images are shown in Fig. 4(b). SEM examinations reveal that the compound layer has a uniformly homogeneous microstructure under all nitriding conditions. They also reveal an affected layer, called the diffusion layer [3–14], inside the compound layer. Furthermore, Fig. 4(b) shows that the compound layer of all specimens consists of two different layers, an outer layer labeled A and an inner layer labeled B. The thickness of the compound layer in Ti–50Al and Ti–53Al is thinner than in Ti–25Al and Ti–40Al. Layer B in Ti–25Al and Ti–40Al is a small fraction of the whole compound layer, but in Ti–50Al and Ti–53Al it is a large fraction. The reason for this feature will be discussed in Section 3.5.

The microstructure of the diffusion layer is strongly dependent on the alloy composition and ion-nitriding conditions. The diffusion layer of Ti–25Al consists of several different layers, as shown in Fig. 3. However,

Fig. 3. Optical micrographs of cross-sections of samples ion nitrided at 1000 °C for 12 h and 8 Torr with $[N_2]/[H_2]=10$: CL; compound layer; DL; diffusion layer.

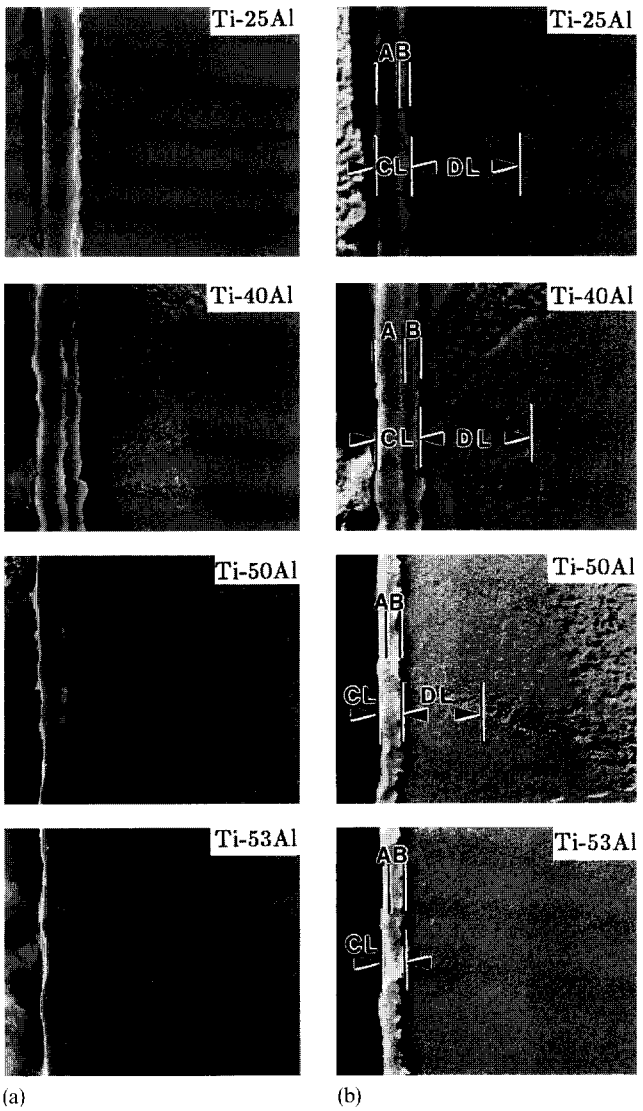

Fig. 4. Scanning electron micrographs of cross-sections of samples ion nitrided at 1000 °C for 12 h and 8 Torr with $[N_2]/[H_2]=10$ sharing (a) a secondary-electron image and (b) a backscattered electron image: CL, compound layer; DL, diffusion layer.

these different layers are easily attacked by the etching reagent, as shown in Fig. 4(b). The diffusion layer of Ti–40Al is not the original laminar structure, as shown in Figs. 3 and 4. In Fig. 4, the diffusion layer of Ti–53Al is not distinguishable, compared with Ti–50Al. Under identical ion-nitriding conditions, the depth of diffusion layer is thicker in Ti–25Al and Ti–40Al than in Ti–50Al and Ti–53Al. This feature is different from that which occurs in titanium alloys; in such alloys, increasing aluminum concentrations can enhance the nitrogen diffusion rate [12]. Here, in titanium aluminides, the solubility of nitrogen in the α_2-Ti_3Al phase is larger than in the γ-TiAl phase [19]. At the same time, the affinity between titanium and nitrogen is greater than that between aluminum and nitrogen [20]. Therefore, in titanium-rich aluminides (e.g. Ti–25Al and Ti–40Al), the nitrogen diffusion layer can extend much further than that in titanium-poor aluminides (e.g. Ti–50Al and Ti–53Al). The ion-nitriding mechanism will be further discussed in Section 3.5.

XRD results shown in Fig. 5 indicate that the nitrided layer is mainly composed of TiN and Ti_2AlN. Ti_2N has not been found in nitrided aluminides, even when the sample was nitrided at short time intervals (4 h) and low temperature (700 °C) [21]. From Fig. 5, the intensity of Ti_2AlN relative to TiN increases as the aluminum content increases. Also, the intensity of the Ti_2AlN peak in the compound layer increases with increasing Al content. For example, the intensity ratio of Ti_2AlN to TiN in the compound layer of Ti–25Al is less than that in Ti–53Al. This means that the compound layer of Ti–53Al has a higher content of Ti_2AlN than the compound layer of Ti–25Al does. The details of these experimental results will be further discussed in Section 3.4. Since the Vickers hardness of TiN is higher than that of Ti_2AlN [22], it then follows that, under the same nitriding conditions, the surface hardness of ion-nitrided Ti–25Al is greater than that of Ti–53Al. This is verified by the results shown in Fig. 2.

3.3. Compositional analysis of compound layer and diffusion layer in ion-nitrided titanium aluminides

The concentration profiles of Ti, Al and N in the ion-nitrided layers of all specimens were examined by electron probe microanalysis (EPMA) (using a 1 μm width probe). These data are shown in Fig. 6. In order to obtain a precise composition analysis, the surface of the mounted specimens was carefully polished without any etching. For Ti–25Al and Ti–40Al, the intensity of the N Kα line increases from the surface to a maximum at the position of the outer compound layer (layer A). It then decreases continuously through the B layer, gradually leveling off in the diffusion layer. For Ti–50Al and Ti–53Al, the intensity of the N Kα line increases from the surface to a maximum at the interface of layers A and B. It then decreased continuously. From Fig. 6, it is obvious that the thickness of diffusion layer for all specimens is not easy to measure, because of the rapid flattening of the N Kα curve in the diffusion layer. The intensity of the Ti Kα line for all specimens also increases from the surface to a maximum at the A–B interface. The Ti Kα curve then gradually drops in the layer B, reaching a minimum at the interface of layer B and the diffusion layer (as indicated by arrows in Fig. 6). The intensity then levels off in the diffusion layer. The Al Kα intensity is quite low in layer A and is closely related to the Al content of samples. For Ti–25Al and Ti–40Al alloys, the intensity of the Al Kα line in layer A is rather weak. It increases from layer B to a maximum at the diffusion layer, showing at the same time large intensity variations. For Ti–50Al and Ti–53Al, the intensity of

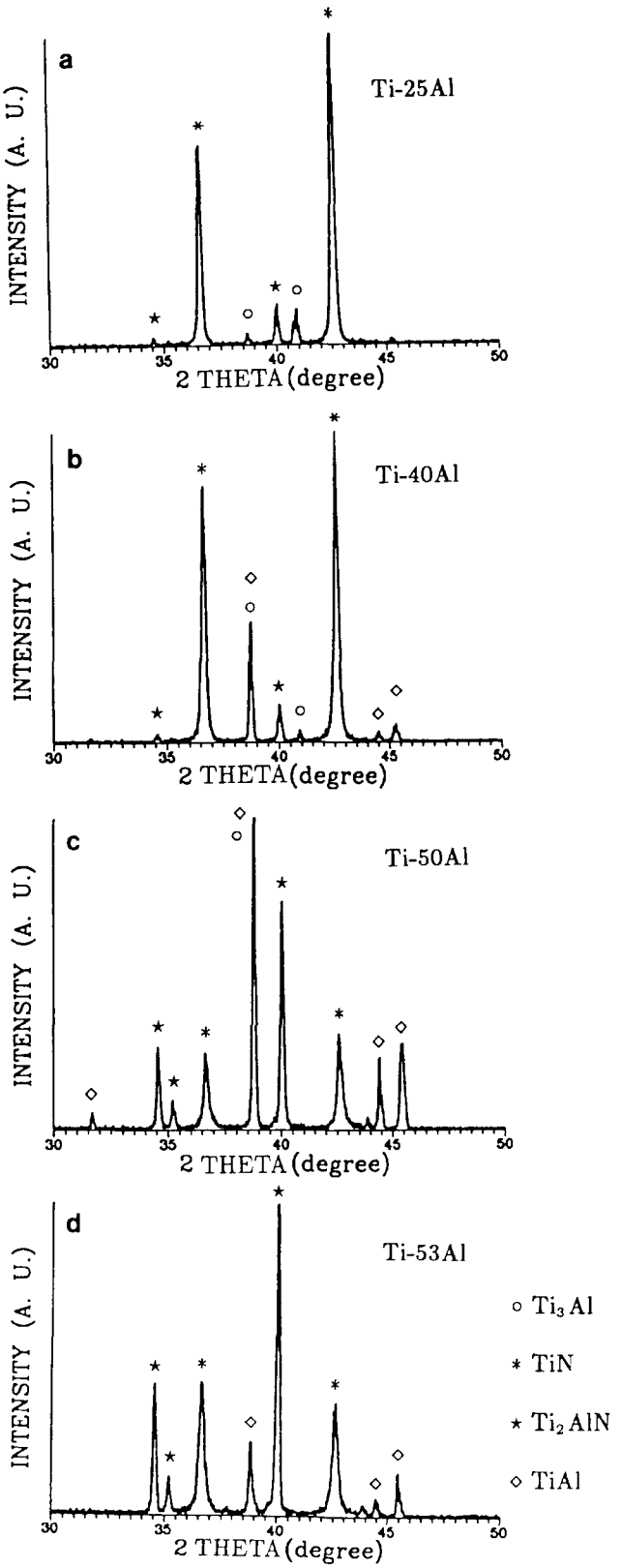

Fig. 5. XRD patterns of samples ion nitrided at 1000 °C for 12 h and 8 Torr with $[N_2]/[H_2]=10$ (All., arbitrary units): (a) Ti–25Al; (b) Ti–40Al; (c) Ti–50Al; (d) Ti–53Al.

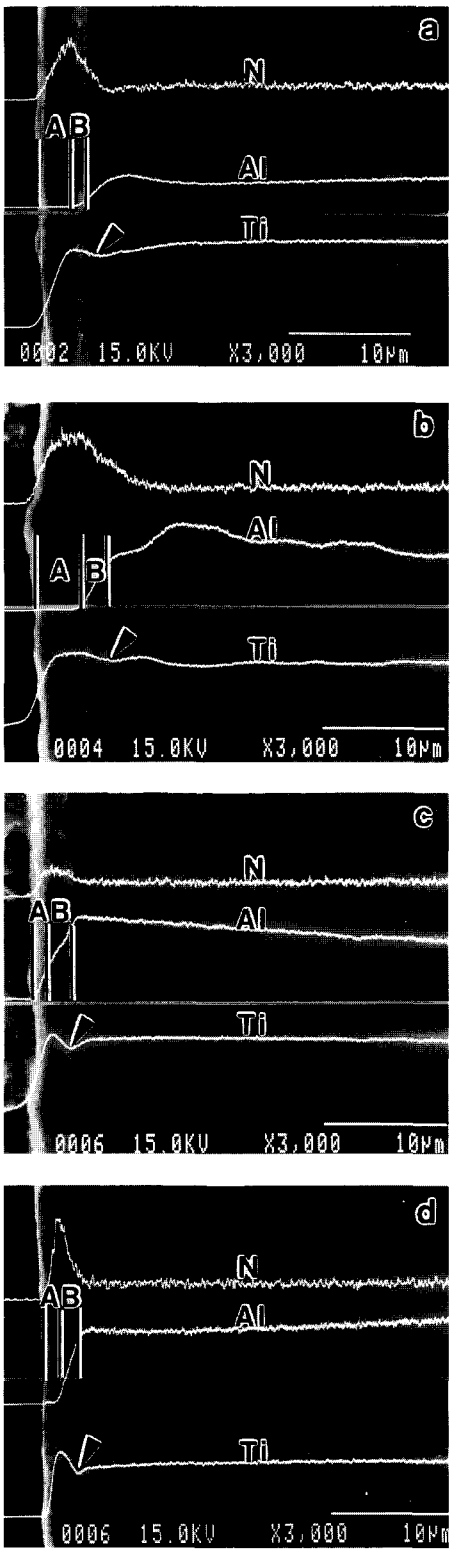

Fig. 6. EPMA line scan of samples ion nitrided at 1000 °C for 12 h and 8 Torr, with $[N_2]/[H_2]=10$: (a) Ti–25Al; (b) Ti–40Al; (c) Ti–50Al; (d) Ti–53Al.

Table 2
The strongest intensities of the peak lines of the identified phases as a function of nitriding temperature for Ti–25Al and Ti–53Al

Nitriding temperature (°C)	Intensity of X-ray peak for identified phase							
	Ti_2AlN					TiN		
	(100)	(103)	(106)	(110)	(116)	(111)	(200)	(220)
Ti–25Al								
1000	1.8	10.5	2.2	27.9	1.5	64.0	100	42.6
900	–	3.3	0.6	7.0	0.5	100	30.3	12.8
800	–	4.7	–	–	–	19.1	20.9	8.7
Ti–53Al								
1000	39.7	100	5.7	39.7	12.6	41.6	33.3	39.7
900	1.7	5.5	0.4	1.5	0.4	1.1	0.7	1.5
800	1.5	7.0	–	–	–	4.3	2.5	1.6

the Al Kα line increases from the surface to the interface of the compound layer and diffusion layer and then levels off in the diffusion layer. From the results in Fig. 5 as well as the Al and N concentration variations shown in Fig. 6, we propose that a TiN compound forms in layer A and a Ti_2AlN compound forms in layer B. As mentioned above and shown by arrows in Fig. 6, the Ti concentration has a shallow dip at the interface of layer B and the diffusion layer. This feature may be attributed to the difference between the chemical affinity of Ti and N and that of Al and N, as described in Section 3.5.

From Fig. 6, Al and Ti, but not N, show concentration variations in the diffusion layer. This means that the nitrogen can diffuse to the compound layer but very little can diffuse to the diffusion layer. According to Part II of this study [23], the difference between the etching speeds of α_2 and γ titanium aluminides [24], as well as the variation in Al and Ti elements in the diffusion layer, results in different etching speeds and therefore different contrasts during microscopy, as observed in Figs. 3 and 4.

3.4. The ratio of TiN to Ti_2AlN formed in the ion-nitrided layer

As mentioned in Section 3.2, TiN and Ti_2AlN are the main phases in the ion-nitrided layer of titanium aluminides. The ratio of TiN to Ti_2AlN in the nitrided layer is related to the Al content of the material. In order to understand how much TiN and Ti_2AlN are formed in the nitrided layer, the following method was used to compare the ratio of these different phases. We assumed the power of the incident X-ray beam and the method of sample holding to be identical (i.e. the areas projected by the incident X-ray beam are identical in each XRD experiment). Because the orientation of TiN and/or Ti_2AlN crystals in the nitrided layer has a random distribution, following the method of [3], we can take the strongest intensity of the diffraction peaks of TiN and Ti_2AlN phases as the reference peak to compare the relative amounts of these phases in the nitrided layer. Following this method, we tested the specimens used in Fig. 2. Typical experimental results are shown in Tables 2 and 3.

In Table 2 the results are listed for Ti–25Al and Ti–53Al. The samples were ion nitrided at 8 Torr, $[N_2]/[H_2]=10$ and 12 h for various nitriding temperatures. For Ti–25Al the ratio of the TiN(200) peak to the Ti_2AlN(103) peak at 800 °C for 12 h is approximately 4.4 (20.9/4.7), and the ratio of the TiN(200) peak to the Ti_2AlN(110) peak at 1000 °C for 12 h is approximately 3.6 (100/27.9). For Ti–53Al, however, the ratio is 0.61 (4.3/7.0) for the former case and is 0.42 (41.6/100) for the latter. Table 3 shows the results for Ti–25Al and Ti–53Al, ion-nitrided at 900 °C, 8 Torr and $[N_2]/[H_2]=10$ for various nitriding times. For Ti–25Al the ratio of the TiN(200) peak to the Ti_2AlN(110) peak at 900 °C for 6 h is approximately 2.6 (100/37.8), and the ratio of the TiN(111) peak to the Ti_2AlN(110) peak at 900 °C for 24 h is approximately 3.9 (100/25.9). For

Table 3
The strongest intensities of the peak lines of the identified phases as a function of nitriding time for Ti–25Al and Ti–53Al

Nitriding time (h)	Intensity of X-ray peak for identified phase							
	Ti_2AlN					TiN		
	(100)	(103)	(106)	(110)	(116)	(111)	(200)	(220)
Ti–25Al								
24	1.0	6.6	1.2	25.9	1.0	100	40.5	30.1
12	–	3.3	0.6	7.0	0.5	100	30.3	12.8
6	2.3	14.1	2.1	37.8	–	83.9	100	37.8
Ti–53Al								
24	8.0	21.6	1.2	6.4	2.8	4.3	2.2	9.6
12	1.7	5.5	0.4	1.5	0.4	1.1	0.7	1.5
6	2.3	9.0	0.6	2.0	0.7	1.7	1.5	2.0

Ti–53Al, however, the ratio is 0.22 (2.0/9.0) for the former case and is 0.44 (9.6/21.6) for the latter. These data indicate that TiN forms more easily in Ti–25Al, while Ti_2AlN forms more easily in Ti–53Al. The TiN formation is strongly dependent on temperature in Ti–25Al, while TiN and Ti_2AlN formation are both dependent on temperature in Ti–53Al.

3.5. *Ion-nitriding mechanism in titanium aluminides*

The detailed reaction mechanism in the ion-nitriding process has not been clarified yet; however, two mechanisms have been proposed to explain the ion-nitriding process in steels [25,26]. The first mechanism proposes sputtering of the Fe atoms, gasous reaction and then deposition on the specimen. The second mechanism proposes a surface reaction and then diffusion of nitrogen into the specimen. To explain the ion-nitriding reaction in Ti_3Al and TiAl, we propose the four-step mechanism shown in Fig. 7. When the N^+ ions hit the surface of workpiece, metal atoms (Ti and Al) are detached and the workpiece is heated. At the same time, non-metallic atoms such as carbon and oxygen are also detached. In this way, the surface is freed from oxides, carbides etc., allowing N^+ ions to be sputtered onto the clean surface (Fig. 7(I)). Ti and Al atoms which are detached from the surface can react with the highly reactive nitrogen atoms in the plasma region near the surface of workpiece. Because the chemical affinity of Ti and N is stronger than that of Al and N [20], the combination of an N^+ ion and a Ti atom occurs more easily than that of an N^+ ion and an Al atom. This means that the material deposited on the workpiece surface is composed of a greater amount of TiN than AlN, as shown in layer A of Fig. 7(II). While the sputtering is going on, the titanium atom in TiN and the aluminum atom in AlN can be detached from the deposited surface again. This causes a further reduction in the concentration of AlN in the plasma region. The final result is that TiN becomes the main phase in the outer surface, as shown in layer A of Fig. 7(III). From a collision standpoint, Ti_3Al has relatively more Ti atoms and fewer Al atoms than TiAl; thus N^+ ions have more opportunity to react with Ti than Al in the Ti_3Al. This causes the formation of TiN in ion-nitrided Ti–25Al to be considerably greater than in ion-nitrided Ti–53Al, as shown in the XRD results in Fig. 5. This feature also explains the fact that different amounts of TiN are formed in layer A of Ti_3Al and TiAl, as shown in Figs. 7(II) and 7(III). We believe that the AlN phase was not found in the XRD results (Fig. 5) because the amount of AlN is too small to detect. As the process continues, the sputtered N^+ ions at the interface of layers A and B of Fig. 7(II) diffuse inwards. When N^+ ions diffuse into layer B, the Ti atoms in layer B react more easily with N^+ because the chemical affinity of Ti and N is stronger than that of Al and N [20]. Thus there is a outward driving force for Ti atoms which, together with the inward movement of N^+ ions, forms TiN or Ti_2N and thickens layer A. Al atoms left behind in layer B then react with TiN or Ti_2N to form Ti_2AlN in layer B. As a result, there is a drop in the Ti concentration at the interface of the compound layer and the diffusion layer, as shown by arrows in Fig. 6. Thus, when the aluminum content increases, as in the case of TiAl alloy, the relative amount of Ti_2AlN increases in layer B (Fig. 7(IV)). When the ion-nitriding temperature is increased, the diffusion rates of Ti, Al and N^+ atoms increase, and the XRD intensity of the Ti_2AlN phase also becomes stronger. This feature can be seen in Tables 2 and 3. The amounts of TiN and Ti_2AlN formed in ion-nitriding titanium aluminides are also discussed in Section 3.4.

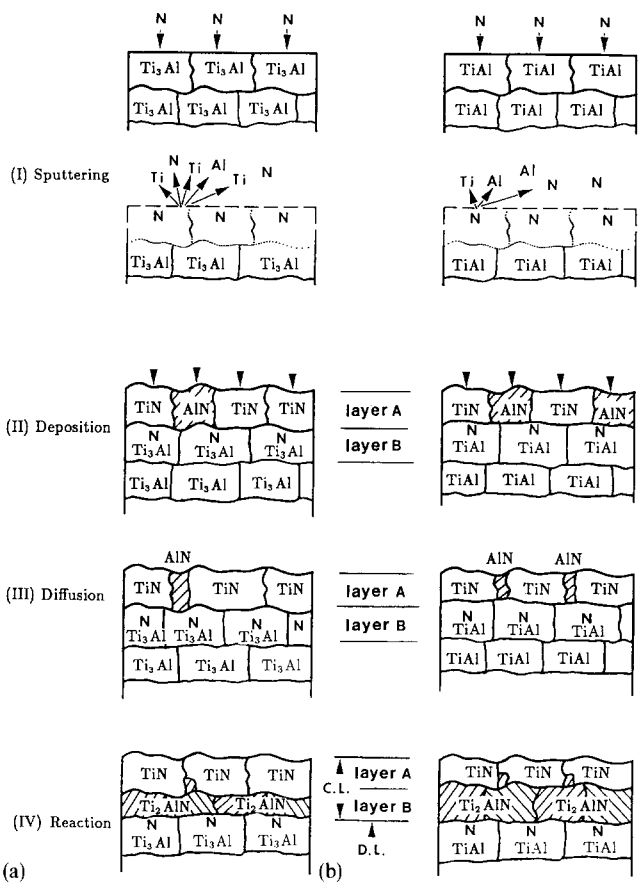

Fig. 7. Schematic diagram of the ion nitriding of (a) Ti_3Al (Ti–25Al) and (b) TiAl (Ti–53Al): CL, compound layer; DL, diffusion layer.

When the TiN in the layer A (Fig. 7) reaches a certain thickness, it can become a barrier [27,28] and subsequently reduce the diffusion of N^+ ions into the matrix. For example, Ti–25Al and Ti–40Al have a thicker (TiN) layer A than do Ti–50Al and Ti–53Al. This feature is reflected in undetectable nitrogen concentrations in the diffusion layers of Ti–25Al and Ti–40Al, and in thin B

layers in these two alloys relative to Ti–50Al and Ti–53Al (Fig. 4(b) and schematically in layer B in Fig. 7(IV)).

4. Conclusions

The ion nitriding of titanium aluminides with 25–53 at.% Al under an N_2–H_2 atmosphere has been investigated. The results obtained by means the orthogonal test, micro-Vickers hardness test, XRD, OM, SEM and EPMA can be summarized as follows.

(1) From the orthogonal test and ANOVA analysis of the four process parameters, namely nitriding temperature, nitriding time, working pressure and $[N_2]/[H_2]$ ratio, the ion-nitriding parameters of titanium aluminides with respect to surface hardness mainly depend on temperature and time.

(2) The nitrided layer consists of the TiN and Ti_2AlN phases in the compound layer. As the amount of Al increases, the XRD intensity of the Ti_2AlN phase becomes stronger. The intensity ratio of Ti_2AlN to TiN in the compound layer of Ti–25Al is less than that of Ti–53Al under the same nitriding condition. Ti–40Al forms the thickest compound layer. The diffusion layer in all cases appears to have little nitrogen which allows this layer to be easily attacked by the etching reagent.

(3) The intensity of TiN is strongly dependent on nitriding temperature in Ti–25Al, while both TiN and Ti_2AlN formation are dependent on nitriding temperature in Ti–53Al.

(4) The ion-nitriding mechanism of titanium aluminides is suggested to include several simultaneous steps: the sputtering of titanium and aluminum from the surface, the deposition of TiN and AlN, the diffusion of N^+ ions into the matrix, the reaction of Ti and N^+ to form TiN, and the reaction of Al and TiN or Ti_2N to form Ti_2AlN.

Acknowledgements

This study was partly supported by the LIO-HO Machine Works, Ltd., Taiwan. The authors are grateful to the Heat Treatment Division of the Metal Industries Research & Development Centre, Kaohsiung, Taiwan, for their kind support in the ion-nitriding experiment and also to Professor R.Y. Lin (National Taiwan University) for his helpful discussions.

References

[1] *ASM Handbook*, Vol. 4, 9th edn, American Society for Metals, Metals Park, OH, 1991, p. 387.
[2] W. Kovacs and W. Russelll, *Proc. ASM Int. Conf. on Ion Nitriding*, American Society for Metals, Metals Park, OH, 1986, p. 9.
[3] L.H. Chang, L.K. Lee, H.C. Peng and C.Y. Wang, *Acta Metall. Sin.*, *20* (1984) A221–A228 (in Chinese).
[4] A. Raveh, P.L. Hansen, R. Avni and A. Grill, *Surf. Coat. Technol.*, *38* (1989) 339–351.
[5] E. Metin and O.T. Inal, *Metall. Trans. A*, *20* (1989) 1819–1832.
[6] E. Metin and O.T. Inal, *Mater. Sci. Eng.*, *A145* (1991) 65–77.
[7] E. Metin, *Scr. Metall.*, *26* (1992) 1193–1197.
[8] H.J. Brading, P.H. Morton, T. Bell and L.G. Earwaker, *Surf. Eng.*, *8* (1992) 206–212.
[9] A. Raveh, R. Avni and A. Grill, *Thin Solid Films*, *186* (1990) 241–256.
[10] F.M. Kustas, M.S. Misra, R. Wei, P.J. Wilbur and J.A. Knapp, *Surf. Coat. Technol.*, *51* (1992) 100–105.
[11] P. Scardi, B. Tesi, T. Bacci and C. Gianoglio, *Surf. Coat. Technol.*, *41* (1990) 83–91.
[12] K.T. Rie and Th. Lampe, *Mater. Sci. Eng.*, *69* (1985) 473–481.
[13] E. Rolinski, *Mater. Sci. Eng.*, *100* (1988) 193–199.
[14] R. Avni and T. Spalvins, *Mater. Sci. Eng.*, *95* (1987) 237–246.
[15] T. Matsushima and K. Saito, *J. Jpn. Inst. Met.*, *57* (1993) 325–331.
[16] K. Saito and T. Matsushima, *Mater. Sci. Eng.*, *A115* (1989) 355–359.
[17] J.C. Pivin, P. Zheng and M.O. Ruault, *Mater. Sci. Eng.*, *A115* (1989) 83–88.
[18] P.J. Ross, *Taguchi Techniques for Quality Engineering*, McGraw-Hill, New York, 1988, p. 23.
[19] M.J. Kaufman, D.G. Konitzer, R.D. Shull and H.L. Fraser, *Scr. Metall.*, *20* (1986) 103–108.
[20] C.E. Wicks and F.E. Block, *Thermodynamic Properties of 65 Elements–Their Oxides, Halides, Carbides, and Nitrides*, US Government Printing Office, Washington, DC, 1963, pp. 13–124.
[21] C.L. Chu and S.K. Wu, unpublished work, 1993.
[22] S. Becker, A. Rahmel, M. Schorr and M. Schutze, *Oxid. Met.*, *38* (1992) 425–464.
[23] C.L. Chu and S.K. Wu, *Surf. Coat. Technol.*, (1995).
[24] A. Takasaki, K. Ojima and Y. Taneda, *Scr. Metall.*, *30*(9) (1994) 1095–1098.
[25] B. Edenhofer, *Heat Treat. Met.*, *1* (1974) 23–26.
[26] T. Spalvins, *Proc. ASM Int. Conf. on Ion Nitriding*, American Society for Metals, Metals Park, OH, 1986, p. 1.
[27] M. Wittmer, *Appl. Phys. Lett.*, *36* (6) (1980) 456–458.
[28] M. Wittmer, *Appl. Phys. Lett.*, *37* (6) (1980) 540–542.